



**Polymer and Magnetic Nanoparticle Composites with
Tunable Magneto-Optical Activity: Role of Nanoparticle
Dispersion for High Verdet Constant Materials**

Journal:	<i>Journal of Materials Chemistry C</i>
Manuscript ID	TC-ART-01-2020-000077.R1
Article Type:	Paper
Date Submitted by the Author:	06-Mar-2020
Complete List of Authors:	<p>Pavlopoulos, Nicholas; University of Arizona, Chemistry & Biochemistry; Technion Israel Institute of Technology, Chemistry</p> <p>Kang, Kyungseok; University of Arizona, Department of Chemistry and Biochemistry</p> <p>Holmen, Lindsey; University of Arizona, Department of Chemistry and Biochemistry</p> <p>Lyons, Nicholas; University of Arizona</p> <p>Akhoundi, Farhoud; University of Arizona</p> <p>Carothers, Kyle; University of Arizona, Chemistry</p> <p>Jenkins, Shelbi; University of Arizona</p> <p>Lee, Taeheon; University of Arizona</p> <p>Kochenderfer, Tobias; University of Arizona</p> <p>Phan, Anthony; University of Arizona</p> <p>Phan, David; University of Delaware, Materials Science & Engineering</p> <p>Mackay, Michael; University of Delaware, Department of Materials Science and Engineering Engineering</p> <p>Shim, In-Bo; Kookmin University, Nano and Electronic Physics</p> <p>Char, Kookheon; Seoul National University, Center for Functional Polymer Thin Films</p> <p>Nasser, Peyghambarian; University of Arizona</p> <p>LaComb, Lloyd; University of Arizona</p> <p>Norwood, Robert; University of Arizona, Optical Sciences</p> <p>Pyun, Jeff; University of Arizona, Chemistry</p>

ARTICLE

Polymer and Magnetic Nanoparticle Composites with Tunable Magneto-Optical Activity: Role of Nanoparticle Dispersion for High Verdet Constant Materials

Received 00th January 20xx,
Accepted 00th January 20xx

DOI: 10.1039/x0xx00000x

Pavlopoulos, N. G.^{a,b}; Kang, K. S.^a; Holmen, L.N.^a; Lyons, N.P.^c; Akhoundi, F.^c; Carothers, K.J.^a; Jenkins, S.L.^c; Lee, T.^a; Kochenderfer, T.M.^a; Phan, A.^a; Phan, D.^d; Mackay, M.E.^d; Shim, I.^e; Char, K.^e; Peyghambarian, N.^c; LaComb L. J.^c; Norwood, R.A.^c; Pyun, J.^a

We report on a new strategy for preparing polymer-nanoparticle composite Faraday rotators for use in magnetic sensing and optical isolation. While most applications of Faraday rotators make use of inorganic garnet crystals, these are generally limited by low magneto-optical activity (low Verdet constants), high cost, and/or limited processing options. This has led to an interest in new materials with improved activity and processing characteristics. We have developed a new type of magneto-optical material based on polymer-nanoparticle composites that can be completely prepared by solution processing methods with tunable Verdet constants and device sensitivity. By exchanging native surface ligands on magneto-optically active CoFe₂O₄ nanocrystals with polymer compatible ligands, enhanced nanoparticle dispersion in processible polymer matrices was observed at up to 15 wt% inorganic loading. Employing a multilayer polymer film construct, functional Faraday rotator devices were prepared by simple sequential spin-coating of active nanocomposite and protective, barrier cellulose acetate layers. For these assemblies, magneto-optic activity and sensitivity are easily tuned through variation of nanoparticle feed and control of polymer film layers, respectively. These multilayered Faraday rotators show up to a 10-fold enhancement in Verdet constant compared to reference terbium gallium garnets at 1310 nm, opening new possibilities for the fabrication of “plastic garnets” as low cost alternatives to existing inorganic materials for use in the near-IR.

1. Introduction

Magneto-optically active materials are ubiquitous in photonic devices, as optical isolators, optical circulators, optical switches, magneto-optic (MO) modulators, and high performance magnetic field sensors.¹⁻⁶ In particular, optical isolators find extensive use in commercial high powered laser and communications systems, preventing unwanted feedback of reflected light into the source resonant cavity.⁷ The Faraday effect, discovered by Michael Faraday in 1845, is one of the fundamental MO effects, describing the influence of an applied magnetic field on polarized light passing through an MO active material. By application of a magnetic field parallel to the direction of light propagation, a rotation of the polarization plane of linearly polarized light is observed, due to a field induced circular birefringence along the axis of the applied field.^{1, 8-10} The extent of this effect for a material is quantified by the material's Verdet constant (V), which is a wavelength and temperature dependent constant; the resulting polarization rotation (θ) is the

product of V , the applied magnetic field (B) and the path length of light through the material (L), as shown in equation 1.

$$\theta = VBL \text{ (eq. 1)}$$

In particular, for optical isolation and magnetic sensing, large path lengths and high Verdet constants are needed, to enable orthogonal polarization/extinguishing of reflected beams and sensitive magnetic field detection, respectively.⁷ The most common enabling material for these applications in the visible to near infrared (NIR) window is terbium gallium garnet (TGG, Tb₃Ga₅O₁₂; $V_{TGG} = 2.2 \times 10^3$ °/Tm at 1310 nm)¹¹⁻¹⁵. While these ferromagnetic, rare-earth based crystals are highly stable and transparent, these materials are limited by modest Verdet constants and substantial temperature dependence. Furthermore, these materials are often prepared as single crystals to enable millimeter to centimeter path lengths, for which device fabrication and integrated photonic applications are challenging owing to the crystallinity of the rotators.^{11, 16}

^a Department of Chemistry & Biochemistry, University of Arizona

^b Schulich Faculty of Chemistry, Technion – Israel Institute of Technology

^c Wyant College of Optical Sciences, University of Arizona

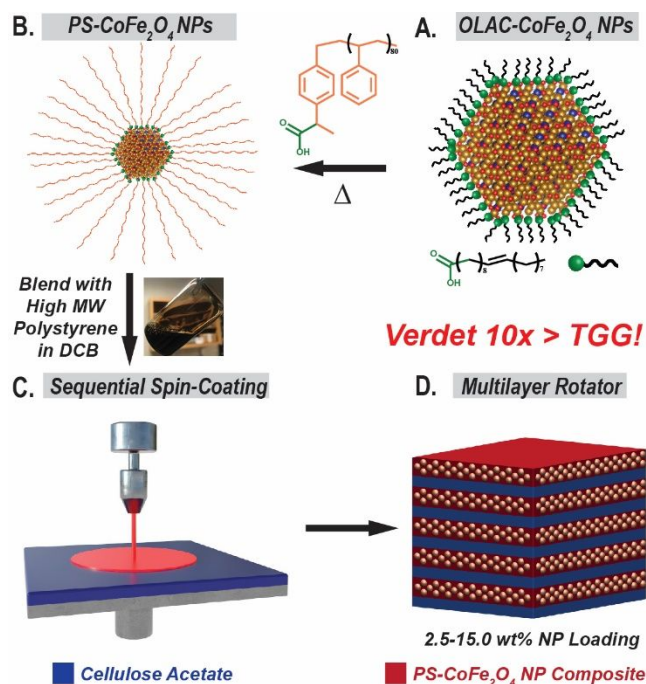
^d Department of Chemical Engineering, University of Delaware

^e Department of Nanoscale Physics, Kookmin University

Electronic Supplementary Information (ESI) available: [details of any supplementary information available should be included here]. See DOI: 10.1039/x0xx00000x

An important challenge that remains for the fabrication of low-cost alternatives to traditional garnet crystals is the creation of processable materials with both high Verdet constants and high transparency, especially in the NIR. To this end, substantial efforts have been made in the past decade to develop polymer based analogues to the ferromagnetic garnets, with semiconducting polymers and nanoparticle-polymer composite systems being most widely explored. Multiple groups have reported on the strong Faraday effect exhibited by polythiophene based systems, with recent work by Swager et al. demonstrating high Verdet constants of up to 7.6×10^4 °/Tm for sulfone-containing chiral helical polythiophenes at 532 nm.¹⁷ Additionally, Prasad and co-workers recently reported on tuning MO activity by doping organic biradicals into polyfluorene chiral helical polymers, obtaining Verdet values of up to 3.8×10^5 °/Tm at 410 nm.¹⁸ These studies point to strong effects of nanoscopic ordering and architecture on MO activity, and provide principles for the design of polymer systems with high Verdet constants. However, the wavelength dependence of the MO activity for these systems often requires measurements at values proximal to absorption bands. Additionally, difficulty in scaling and processing of these all-organic systems to support thick films (> 1 μm) with large rotations limits their application and often requires high fields for measurement (0.5-1.5 T).

An alternative, low-cost approach towards materials with improved Faraday rotation involves the incorporation of high Verdet nanoparticles (NPs) into polymer matrices to generate MO active nanocomposites. These materials have the advantage of potentially high Verdet constant values off-resonance from primary absorption bands due to the tunable properties of the MO active nanoparticles. However, while the classical magnetic properties of single domain isolated nanoparticles are well understood, correlating single particle effects to MO properties is a new area of research in need of precise model systems to unravel the materials physics of these systems. For this application, various systems have been explored, most often incorporating magnetic nanoparticles (Co, $\gamma\text{-Fe}_2\text{O}_3$, Fe_3O_4 , CoFe_2O_4 , FePt)¹⁹⁻²³ into sol-gel or polymer matrices. While wholly inorganic composites are superior in terms of matrix stability, porosity induced scattering has been shown to limit the performance of sol-gel and inverse opal based systems.²⁴⁻²⁷ Additionally, aggregation of nanoparticles in polymer-nanoparticle composites at appreciable loadings (> 1 wt% loading) severely limit the Faraday effect in these materials at reasonable length scales for most applications. Despite these challenges, recent efforts to improve nanoparticle dispersion in polymer matrices by surface functionalization of magnetic nanoparticles enabled fabrication of relatively thick films with high Verdet constant values in the NIR. Peyghambarian and coworkers demonstrated Verdet constants of up to 8.0×10^4 °/Tm at 1310 nm for polymethylmethacrylate (PMMA) grafted Fe_3O_4 nanoparticles (D = 15 nm) crosslinked in a PMMA matrix.^{19, 20, 22, 28} While thick films could be prepared for these materials by melt-processing (> 50 μm), loss of MO activity has been observed over time for Fe_3O_4 based materials, limiting their practical utility.¹⁴ A similar approach was recently employed to prepare polybenzylmethacrylate (PBMA) grafted CoFe_2O_4 nanoparticle (D = 20 nm) composites, however these samples exhibited relatively lower Verdet constant values of 2.2×10^3 °/Tm at 1310 nm.^{19, 22}



Scheme 1. General scheme for the fabrication of Bragg-reflector inspired multilayer Faraday rotators. (A) Oleic acid stabilized CoFe_2O_4 nanoparticles are first ligand exchanged with carboxylic acid terminated polystyrene ligands (MW = 8400 g/mol) to result in (B) PS- CoFe_2O_4 NPs. These particles are subsequently blended with high molecular weight polystyrene in 1,2-dichlorobenzene (DCB) to result in a homogeneous ink. (C) Through a sequential spin coating process, layers of cellulose acetate (thickness = ~ 200 nm) and PSCOOH- CoFe_2O_4 -NP composite (thickness = ~ 1000 nm) are consecutively deposited onto an Au-coated substrate to result in (D) a novel multilayer faraday rotator with tunable total rotation (thickness variation) and Verdet constant (NP loading variation).

Recently, Watkins and coworkers reported the preparation of MO active nanocomposites with enhanced Faraday rotation and dispersion qualities by the incorporation of gallic acid functionalized FePt nanoparticles into polystyrene-block-poly-2-vinylpyridine templates, allowing for high nanoparticle loadings of up to 10 wt% into the final multilayer films. Through variation of nanoparticle size (D = 1.9-9.3 nm) and loading (0.1 – 10.0 wt%), Faraday rotations could be tuned from $0.98 - 2.79 \times 10^4$ °/Tm at 1310 nm for these self-assembled thin films.²¹

While these seminal reports point to the potential for high Verdet composites prepared from magnetic nanoparticles, there is a clear need for robust and versatile methods to functionalize magnetic NPs with ligands to promote dispersion into polymeric media. A number of methods for the preparation polymer-magnetic nanocomposites, or post-functionalization with functional copolymers onto magnetic NPs have been explored and recently reviewed.²⁹⁻³⁴ Furthermore, for the construction of thicker films to enable appreciable optical rotation, the development of process methods to fabricate free standing films of tunable thickness and Faraday rotation remains an important challenge. This type of high Verdet constant nanocomposite would be an attractive alternative to the state-of-the-art garnet materials for MO devices and requires model systems to map the numerous variables of the nanocomposite system (e.g., NP composition, size, surface functionalization, polymeric ligands,

processing methods) required to optimize Faraday rotation. We previously demonstrated that end-functional polymeric ligands prepared by atom transfer radical polymerization (ATRP) are capable of promoting the growth of well-defined ferromagnetic cobalt NPs³⁵⁻³⁷ and functionalization reactions via ligand exchange onto CoNPs.³⁸ However, the use of the end-functional polymeric ligands has not been applied to functionalization and dispersion of magnetic NPs for use in MO applications. Such an approach would allow for modular variation of both NP and polymeric components, and would enable the study of new model systems and device fabrication methods.

Herein, we report on the fabrication of MO active polymer-nanoparticle composite films via solution processing methods that achieve a maximum Verdet constant up to ten-fold greater than commercially available TGG crystals in the NIR region. Furthermore, through variation of nanoparticle loading between 2.5-15.0 wt%, the ability to tune Verdet constants from $\sim 4.2 \times 10^3$ °/Tm to $\sim 2.2 \times 10^4$ °/Tm at 1310 nm has been demonstrated. The key to preparing these devices was synthetic access to superparamagnetic, 5 nm CoFe_2O_4 NPs functionalized with carboxylic acid terminated polystyrene ligands (PS-COOH) which enabled their dispersion in high molecular weight polystyrene matrices with filler loadings well above that of small molecule oleic acid coated NPs. While traditional solution processing has been used to prepare polymer and polymer/nanoparticle composite thin-films for study of their MO properties,^{17, 39-42} characterization of these films often requires strong fields (> 1 T) due to the low interaction pathlength (usually on the order of hundreds of nanometers), preventing use of these materials as optical rotators or in high sensitivity magnetic field sensing. To circumvent this issue, we demonstrate the fabrication of a one-dimensional photonic crystal inspired constructs, which enabled devices of tunable thickness to be designed and studied in low fields (1-7 mT). These alternating layered polymer films were prepared by sequential spin coating of high Verdet constant NPs nanoparticle loaded polystyrene films, followed by deposition of low Verdet constant cellulose acetate layers from orthogonal solvents. To our knowledge, this represents the first report of using this synthetic and processing strategy to fabricate MO active films of precisely tunable Faraday rotation.

The general strategy for the preparation of CoFe_2O_4 -NP based devices with tunable Verdet constants comprised of a four step process enabled by 1) exchange of CoFe_2O_4 surface ligands for a polymer-matrix compatible ligand and 2) a sequential spin coating approach for film processing to prepare layered alternating nanocomposite films (Scheme 1). Through replacement of native nanoparticle ligands for PS-COOH ligands, polymer-nanoparticle composites with nanoparticle loadings of up to 15 wt% could be achieved with minimal scattering induced losses to MO properties. Additionally, through sequential spin coating of high Verdet constant PS- CoFe_2O_4 composite layers and low Verdet constant cellulose acetate layers, devices with high Verdet constant and appreciable thicknesses (5-30 microns) could be prepared.

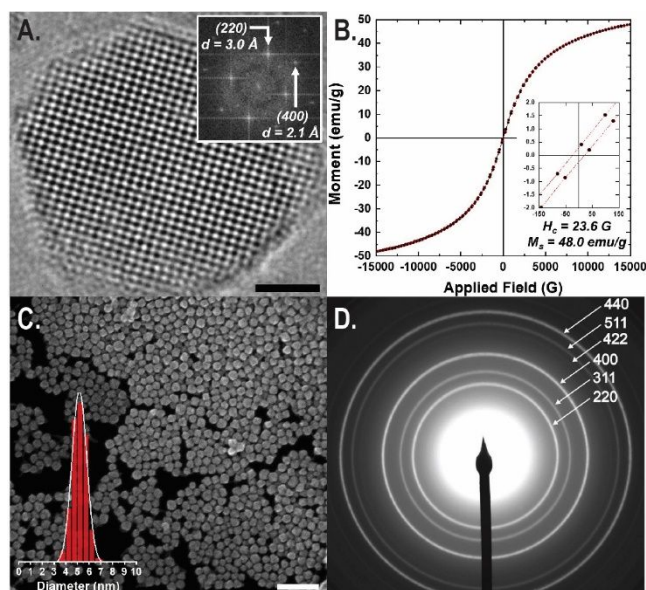


Figure 1. Characterization of 5 nm CoFe_2O_4 nanoparticles. (A) HAADF-STEM imaging demonstrating uniform particle morphology and narrow size distribution (scale bar is 50 nm), (B) SAED pattern for close-packed nanoparticles, demonstrating characteristic patterns for spinel phase CoFe_2O_4 , (C) HRTEM image of a single CoFe_2O_4 nanoparticle along the [001] zone axis (scale bar is 1 nm), with inset FFT demonstrating expected d -spacing for (220) and (400) lattice planes, and (D) VSM measurement demonstrating expected superparamagnetic behavior for the synthesized CoFe_2O_4 nanoparticles.

2. Experimental

2.1 Synthesis of CoFe_2O_4 Nanoparticles

In the first step of this process, superparamagnetic CoFe_2O_4 NPs were prepared as the high Verdet constant component of the Faraday rotating materials. Whereas magnetite NPs have been studied for their high optical transparency in the NIR, they have been observed to lose their MO properties over time, presumably due to the gradual phase change of Fe^{3+} to Fe^{2+} , and resulting spin differences.¹⁴ In contrast, CoFe_2O_4 NPs have been observed to exhibit long term MO stability, due to replacement of the tetrahedral Fe^{2+} species for Co^{2+} in the spinel structure.¹⁹ In order to limit scattering and maximize dispersion in nanocomposite films, small, uniform superparamagnetic NPs (~ 5 nm in size) were targeted as a model system. The CoFe_2O_4 NPs used herein were prepared via a modified method of Lu et al.⁴³ in which cobalt and iron oleate precursors are mixed with oleic acid as the NP ligand stabilizer in benzyl ether at elevated temperature (295 °C) for 1 hour. This process afforded up to 500 mg batches per reaction, which was sufficient quantities for further ligand exchange reactions with polymeric ligands and subsequent solution processing into layered films. More information on the synthetic protocol is provided in the ESI.

2.2 Nanoparticle Characterization

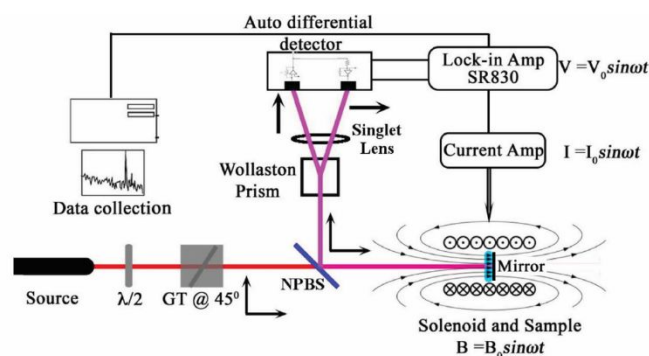
Transmission electron microscopy (TEM) analysis was carried out on the as-synthesized oleic acid coated CoFe_2O_4 NPs to investigate nanoparticle size and morphology. Detailed manual

sizing was performed on these nanocrystals (Figure 1), with Gaussian statistics revealing an average size of 5.2 nm with a narrow distribution (standard deviation of 0.54 nm, $n = 334$). To further confirm the phase of the synthesized NPs, selected area electron diffraction (SAED) analysis was performed, revealing diffraction rings with d-spacings corresponding to those of spinel phase cobalt ferrite (Figure 1b). Additionally, single particle analysis was carried out through high resolution TEM (HR-TEM) and fast Fourier transform (FFT) of the imaged NPs, for which lattice spacings corresponding to the (220) and (400) planes were observed.⁴³ To confirm the expected superparamagnetic properties of the synthesized CoFe_2O_4 NPs, vibrating sample magnetometry was performed at 300 K (Figure 1d), revealing a saturation magnetization of 48.0 emu/g and coercivity of 23.6 gauss, which was consistent with previous reports on the size dependent magnetic properties of CoFe_2O_4 NPs.⁴⁴

2.3 Ligand Exchange of CoFe_2O_4 Nanoparticles

As alluded to earlier, a key step in the preparation of MO active composites was the exchange of native oleic acid ligands for low molecular weight polymeric ligands. Due to the low cost and high degree of synthetic control afforded by oleic acid ligands, their use in colloidal NP preparations is ubiquitous. However, attempts to incorporate oleic acid coated CoFe_2O_4 NPs into optical polymers (i. e. poly(methyl methacrylate) or polystyrene) at appreciable loadings fractions (> 1 wt%) (via blending or forced precipitation) resulted in substantial aggregation and loss of MO properties. Watkins and coworkers have demonstrated improved nanoparticle dispersion in poly-2-vinylpyridine polymer matrices through use of enthalpically favorable hydrogen bonding interactions of surface ligands with polymer sidechains.²¹ However, it would be desirable to have modular compositional variation of polymeric ligands to enable diverse functionalization of magnetic NPs with inexpensive polymeric materials. To this end, we envisioned the use of a low-molecular weight, end-functional polymer ligand prepared from atom transfer radical polymerization (ATRP) would enable efficient functionalization of NPs and further promote dispersion in polymeric films.

In our earlier work, we have demonstrated the use of a carboxylic acid terminated polystyrene (PS-COOH) ligand synthesized via ATRP as the sole ligand in the synthesis of metallic cobalt and cobalt oxide NPs.^{36, 37, 45, 46} This ligand coating enabled excellent solution dispersion of the resulting cobalt and cobalt oxide nanoparticle assemblies. However, initial attempts to synthesize CoFe_2O_4 NPs directly using polymer ligands were not successful, resulting in poor control over nanoparticle morphology and size distribution. Previously, exchange of native oleic acid ligands on FeO_x for a variety of carboxylic acid functionalized small molecule ligands at room temperature has been demonstrated via sonication.⁴⁷ Thus, we posited that the native oleic acid ligands on the synthesized CoFe_2O_4 NPs could be exchanged for PS-COOH ligands via a similar approach. For this, low molecular weight ($M_n = 12,000$ g/mol; $M_w/M_n = 1.18$) PS-



Scheme 2. Schematic of the Faraday rotation measurement system used herein. A 1310 nm Fabry-Perot laser used to generate a beam which is passed through a half-waveplate ($\lambda/2$), Glan Thomson polarizer (GT), and through the MO active sample placed in a sinusoidal magnetic field. Black arrows along the optical path denote polarization states. The purple line represents the second pass through the sample after reflecting off a mirrored substrate.

COOH was first synthesized via ATRP as reported previously.³⁷ This polymeric ligand was used for functionalization of the oleic acid coated CoFe_2O_4 NPs ($D = 5.2 \pm 0.5$ nm) in 1,2-dichlorobenzene (DCB), at elevated temperature ($T = 180$ °C) for 1 hour, resulting in a homogeneous brown dispersion. Successful ligand exchange of PS-COOH onto the magnetic NPs was most easily noted by differences in dispersability after surface modification. Whereas the initial oleic acid coated CoFe_2O_4 NPs are highly dispersible in hexanes, the resulting PS coated cobalt ferrite NPs (PS- CoFe_2O_4 NPs) show virtually no dispersion in hexanes (Figure ESI.1). To further confirm the exchange of PS-COOH onto the CoFe_2O_4 NPs, the obtained pellets were analysed via thermogravimetric analysis (TGA), for which the decomposition profile characteristic of PS was observed (Figure ESI.2) and an apparent ligand grafting density of 0.42 ligands/nm² was calculated.

2.4 Nanoparticle-Polymer Composite Preparation

Synthetic accessibility to PS- CoFe_2O_4 NPs enabled the preparation of polymer-nanoparticle composites with tunable inorganic loadings via solution processing. For this, PS- CoFe_2O_4 NPs were dispersed in 1,2-DCB followed by blending with a freshly prepared solution of high molecular weight commercially available polystyrene ($M_w = 350,000$ g/mol) and heating at 105°C for 1.5 hours to promote efficient dispersion and dissolution of the solids, where tuning of NP to linear PS feed ratios enabled control of the inorganic NP content of the final composites between 2.5-15.0 wt% (more details on composite preparation are supplied in the ESI). After homogenization, the polymer-nanoparticle inks were precipitated into methanol (a poor solvent for both PS-coated NPs and the linear PS binder) and dried, resulting in PS- CoFe_2O_4 composites with improved processing characteristics.

2.5 Fabrication of Multilayer Faraday Rotation Films

Spin coating is routinely used as a simple and fast method to prepare uniform thin films of polymer, nanoparticle, and

polymer-nanoparticle composites from dilute solutions for MO characterization.^{15, 17, 21, 39, 42, 48} However, such approaches generally result in materials with maximum pathlengths on the order of a few microns. While this is acceptable for measurement purposes, practical applications often require optically

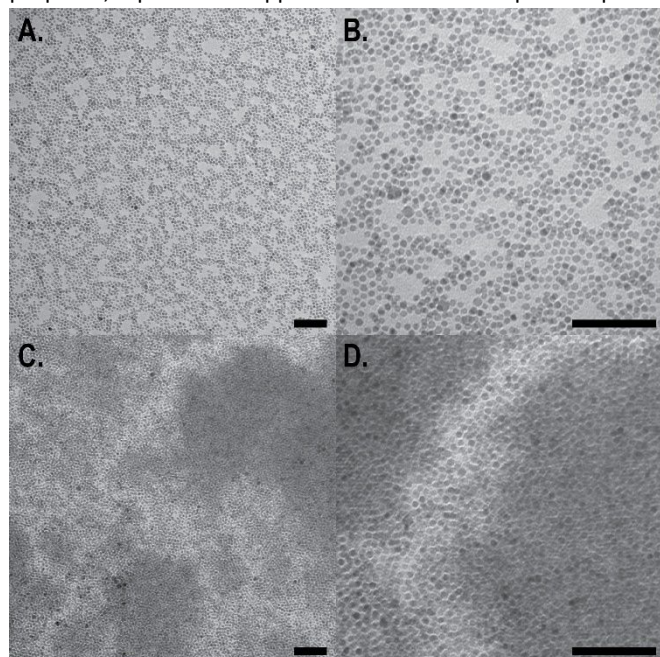


Figure 2. Effect of nanoparticle surface chemistry on dispersion quality in PS-binder matrix. (A) 100 mg/mL dispersion of PS-COOH coated CoFe_2O_4 NPs with PS-binder (scale bar is 100 nm). (B) 100 mg/mL dispersion of PS-COOH coated CoFe_2O_4 NPs with free PS-binder (scale bar is 100 nm). (C) 100 mg/mL dispersion of oleic acid coated CoFe_2O_4 NPs with free PS-binder (scale bar is 100 nm). (D) 100 mg/mL oleic acid coated CoFe_2O_4 NPs with free PS-binder (scale bar is 100 nm).

homogeneous films with path lengths on the order of tens of microns or even millimeters in thicknesses. Achieving such a construct would also enable screening at low magnetic fields (Eq. 1), as opposed to the requisite 0.5 – 1.5 T needed for micron path lengths. Recently, we reported on the use of a modified method of Commereto and Voit et al. to prepare all-polymer one-dimensional photonic crystals via spin coating.^{49, 50} For this, sequential deposition of a low refractive index polymer (cellulose acetate) and high refractive index CHIPs (chalcogenide hybrid inorganic-organic polymers) from orthogonal solvent systems was demonstrated, enabling the preparation of 22-layer films with a total thickness of near 5 microns and high optical quality.⁴⁹ We envisioned a similar approach could be used herein to obtain reasonably thick CoFe_2O_4 nanoparticle films (5-30 microns) through sequential spin coating. To this end, spin curves were developed to obtain thin (~ 200 nm) cellulose acetate (CA) layers, and thick (~ 1000 nm) PS- CoFe_2O_4 layers (detailed fabrication conditions for the multilayer films are included in the ESI).

2.6 Evaluation of Magneto-Optic Activities of Composite Films

The MO activities of the PS- CoFe_2O_4 based multilayer films were evaluated via the experimental setup shown in Scheme 2 and reported in a previous publication.²¹ Briefly, the Verdet

constants were measured in a two-pass sinusoidal magnetic field apparatus using an auto-balanced differential detector with efficient common mode noise cancellation (Nirvana 2017) in conjunction with a lock-in amplifier (Stanford Research Systems SR830). Furthermore, owing to the nonreciprocal nature of Faraday rotation, this two-pass setup generates twice the measurable rotation (θ) for a given magnetic field (B) value, and cancels any rotation that is reciprocal in nature that may result from birefringence or scattering phenomena. At the surface of the multilayer films, a 1-7 mT sinusoidal magnetic flux density was generated by feeding the sinusoidal output of the lock-in amplifier's internal oscillator into a low-noise amplifier/solenoid driver. Further details of the experimental setup and calculation of Faraday rotation are included in the ESI.

3. Results and Discussion

3.1 Morphological Study of Polymer-Nanoparticle Composites

To investigate the morphology of the PS- CoFe_2O_4 NP composites, dispersions were prepared of PS- CoFe_2O_4 NPs and oleic acid coated NPs with blends of linear high molecular weight polystyrene in chlorobenzene, which were drop cast onto carbon coated TEM grids and allowed to dry before imaging. TEM images of the as-prepared composite films cast from solution blends of oleic acid coated and PS- CoFe_2O_4 NPs in the PS matrix at a 10.0 wt% NP loading are shown in Figure 2. In these images, the dark contrast regions represent the individual NPs. For the PS-COOH coated NPs, uniform dispersion of the particles on the grid is observed with minimal NP aggregation and a mean particle diameter of 5.7 ± 0.5 nm ($n = 100$) is observed when dispersed in a PS matrix (Figure 2a,b). These particle sizes are in close agreement with the measured diameter of the initially synthesized oleic acid capped NPs, confirming the fidelity of the ligand exchange process both in maintaining primary particle size and dispersion throughout the composite preparation. In contrast, an identically prepared 10.0 wt% film of oleic acid coated NPs in PS demonstrates substantial aggregation (Figure 2c,d), with regions of phase separation and microscopic aggregation observed throughout the sample when dispersed in a PS matrix. This further affirms the benefit of the described ligand exchange process in preparing homogenous composites. We acknowledge that this approach may not afford optimal NP dispersion in these films, but demonstrates that viability of this approach to enhance nanofiller dispersion using facile processing methods.

3.2 Evaluation of Multilayer Faraday Rotation Film Architecture

To quantitatively study the effect of high Verdet nanoparticle loading on overall Faraday rotation, PS- CoFe_2O_4 composites were prepared with 2.5 wt%, 5.0 wt%, 7.5 wt%, 10.0 wt%, and 15.0 wt% feed ratios (of inorganic CoFe_2O_4 NPs). For convenience, the notation PS- CoFe_2O_4 -x is used to designate a PS-nanoparticle composite film prepared from PS-COOH exchanged CoFe_2O_4 NPs

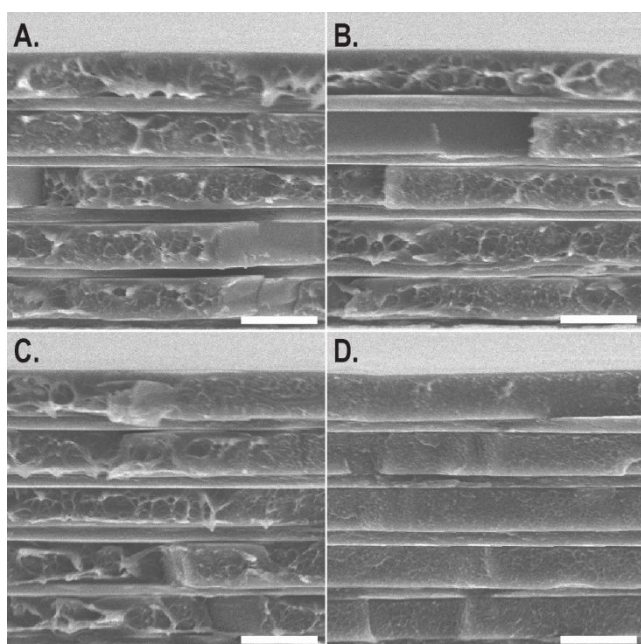


Figure 3. Cross-sectional SEM imaging of multilayer films prepared by freeze fracture with (A) 5.0 wt% feed ratio of CoFe_2O_4 NPs, (B) 7.50 wt% feed ratio of CoFe_2O_4 NPs, (C) 10.0 wt% feed ratio of CoFe_2O_4 NPs, and (D) 15.0 wt% feed ratio of CoFe_2O_4 NPs. All scale bars are 2 microns.

with a total inorganic feed ratio of x -wt%. Recent reports of polymer based Faraday rotation films have demonstrated the convenience of a two-pass device architecture, with MO films being deposited directly onto reflective metal substrates, effectively doubling the total interaction pathlength (and total rotation/device sensitivity at a specific field strength).^{14, 22} As a result, 10 bilayer composite films (five CA and five PS- CoFe_2O_4 layers) were sequentially spin coated onto glass microscope slides coated with 100 nm of vapor-deposited Au (99.5% reflection at 1310 nm), with cellulose acetate being chosen as the first layer to ensure consistency of PS- CoFe_2O_4 layer thicknesses. In this way, each PS- CoFe_2O_4 layer was spin coated atop a previously deposited cellulose acetate layer, the first of which was deposited on the Au-substrate.

The layered film architecture of the assembled CoFe_2O_4 Faraday rotation films was confirmed by cross-sectional SEM imaging (Figure 3). For this, SEM imaging was conducted of freeze fractured multilayered films (further details on freeze fracturing and imaging conditions are included in the ESI), revealing the presence of a well-defined layered morphology of PS- CoFe_2O_4 and cellulose acetate films. The layer contrast in these images may also arise from interfacial charging induced by mild delamination at the layer interfaces upon fracturing (Figure ESI.3). Due to clear resolution of alternating domain boundaries, layer thicknesses could be quantitatively determined and were observed to be within the standard deviation of the expected thicknesses from spin coating methods for both cellulose acetate and PS- CoFe_2O_4 films (see Figure ESI.4 for examples of layer thickness measurements). Furthermore, PS- CoFe_2O_4 thicknesses remained relatively consistent despite varying inorganic content

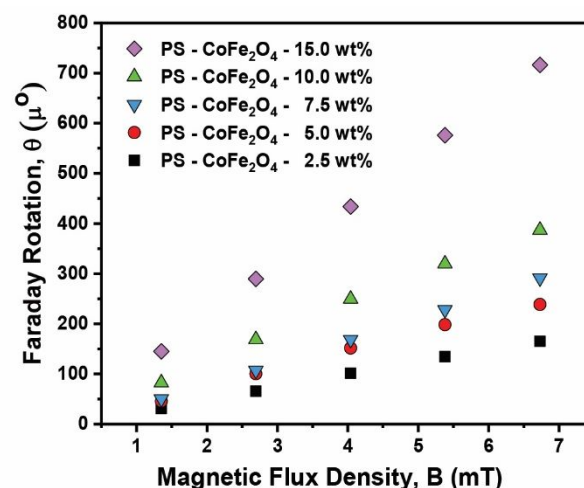


Figure 4. Measurement of total Faraday rotation as a function of magnetic flux density in the 0-7 mT range for PS- CoFe_2O_4 composite based multilayer rotators with varying loadings of CoFe_2O_4 -NPs.

(1026 ± 62 nm), highlighting the reliability of this method for both sample characterization and device fabrication. Interestingly, while layer thicknesses remain consistent, we observed increased surface roughness in some freeze-fractured PS- CoFe_2O_4 layers (Figure 3). We attribute this mechanical damage at the fractured interface to the presence of high energy sites where strain-induced crack propagation could be deflected during freeze-fracturing.

3.3 Performance of Multilayer Faraday Rotator Devices

The MO properties of the multilayer Faraday rotation films were evaluated using a 1310 nm Fabry-Perot laser diode source. As shown in Figure 4, the total rotation of the fabricated devices as a function of magnetic field increases linearly, consistent with expected trends for MO active composites (as per Eq. 1). Previously, it was found that 5.7 nm FePt nanoparticle loading variation had a non-linear effect on the measured Verdet constant in an alternating self-assembled block copolymer system at 1310 nm.²¹ In this system, FePt loading was varied from 0.1 wt% to 10.0 wt%, with measured Verdet values between 0.98×10^4 $^\circ/\text{Tm}$ and 2.21×10^4 $^\circ/\text{Tm}$ at 1310 nm. Surprisingly, herein we find that with increasing NP feed ratio, a significant increase in Verdet constant is observed in the case of PS- CoFe_2O_4 nanoparticle samples, from 4,180 $^\circ/\text{Tm}$ to 21,200 $^\circ/\text{Tm}$. This is surprising, considering the maximum Verdet constant previously reported at 1310 nm for CoFe_2O_4 NPs was on the order of $\sim 2.2 \times 10^3$ $^\circ/\text{Tm}$.¹⁹ We attribute this order of magnitude increase in Verdet constant to the improved dispersion and device architecture employed herein, which served to reduce scattering events and associated losses to MO activity.

To further elucidate the nature of this trend and the effect of NP dispersion on overall MO performance, control devices were prepared from native oleic acid coated CoFe_2O_4 NPs, with near identical NP loadings and layer thicknesses (detailed conditions

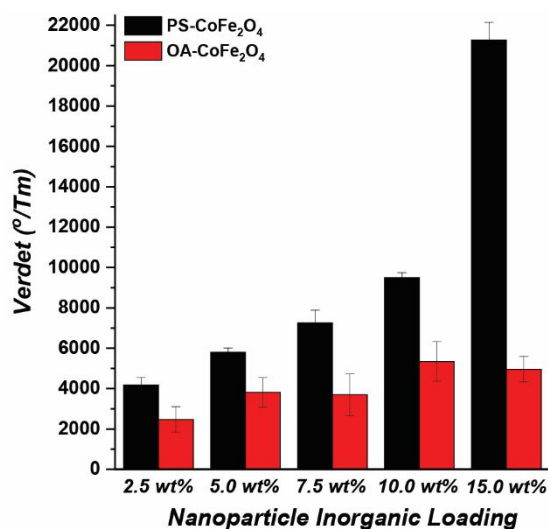


Figure 5. Verdet constant values for each PS-CoFe₂O₄ based composite (black) and oleic acid CoFe₂O₄ based composites (red).

for the preparation of control samples are included in the ESI). As these ligands show poor dispersion quality in polystyrene matrices, substantial aggregation and hazing could be observed in these films. Regardless of nanoparticle loading, all films prepared from oleic acid coated NPs exhibited similar Verdet constants, with maximum rotations of 20 μ degrees and Verdet values of $\sim 4.0 \times 10^3$ deg T⁻¹ m (Figure 5). While this represents an improvement over the Verdet constant of control films of polystyrene, the MO activities of these films are substantially diminished relative to those of surface modified CoFe₂O₄ nanoparticle samples. Based on TEM analysis, the diminished MO activity for the devices prepared from unmodified particles can be correlated to increased aggregation and scattering events in these composites (Figure 2). Effectively, this results in a material that behaves similar to a lower-loading composite, with aggregated regions minimally contributing to the Faraday rotation while resulting in loss of optical transparency.

Furthermore, to quantitatively study the effect of nanoparticle loading on measured device Verdet, TGA analysis was performed on each of the PS-CoFe₂O₄ samples after measurement to assess the actual NP loading in the measured films. By plotting Verdet constant as a function of measured inorganic content, a near linear trend emerges for the dependence of Verdet constant on NP loading in the 2.5-10 wt% inorganic loading range (Figure ESI.5). While similar trends have been observed for high refractive index polymer-nanoparticle composites,⁵¹ to our knowledge this is the first example of composites with predictably tunable Verdet constants as a function of nanoparticle loading, which we attribute to the modularity of our process and the enhanced dispersion arising from the PS-ligand exchange process.

Interestingly, an exponential increase in Verdet constant is observed in the 10-15 wt% inorganic loading range. For Fe₃O₄ NPs dispersed in a PMMA matrix, Smith and coworkers observed a red shift in the Faraday rotation spectrum as a function of

decreased interparticle spacing due to enhanced near-field optical interactions between neighbouring particles, as suggested by discrete-dipole approximation modeling.⁵² For our system, such a shift in peak Faraday rotation would be expected with increased loading, resulting in progressively larger Verdet constants at 1310 nm. The non-monotonic increase between 10-15 wt% thus suggests a critical interparticle spacing, wherein MO activity is maximized. Beyond 15 wt% loading, a marked decrease in MO activity is observed, likely due to aggregation and resultant scattering effects. These results highlight an additional benefit of nanoparticle-polymer composite Faraday rotation materials, wherein interparticle spacing can be tuned to maximized MO activity without inducing aggregation and scattering events, effectively maximizing the Faraday rotation attainable for the composite system. Future work is planned to quantitatively study this interparticle spacing effect on polymer-magnetic nanoparticle composite Verdet constants to further elucidate the non-monotonic increase in Verdet observed in this loading range.

These results suggest nanoparticle dispersion quality plays a significant role on the observed limits to MO activity that can be achieved by increasing nanoparticle loading. By modifying nanoparticle surface chemistry, this limit can be increased by up to an order of magnitude relative to previously reported CoFe₂O₄ systems.¹⁹ This both validates the PS-COOH exchange approach for preparation of highly MO active composite films, and also points to the need to consider not only the “intrinsic” Verdet but also the dispersion of high Verdet fillers in the characterization and reporting of polymer-nanoparticle composite rotators. While similar conclusions have been drawn for obtaining high refractive index composites based on nanoparticle fillers, to our knowledge this is the first extension of this principle to MO active systems.

3.4 Fabrication and Performance of 30-Bilayer Devices

A fundamental advantage of traditional inorganic garnet Faraday rotation materials, such as TGG, is the ability to tune pathlength and thus total rotation at fixed fields with relative ease, enabling sensitive magnetic field sensing and optical isolation. While it is expected that total rotation will increase proportionally with MO active film thickness (Eq. 1), preparation of thick polymer-nanoparticle composites is generally complicated by issues of porosity and aggregation induced scattering events that arise from differential rates of solvent evaporation and monomer curing. To further demonstrate the utility of the sequential spin coating approach developed herein, it was envisioned that the spin coating process could be extended beyond 5-bilayers to facilitate formation of composites with comparable Verdet as their thinner counterparts, but substantially higher total rotation (Figure 6A). For this, the PS-CoFe₂O₄-7.5% sample was chosen, and a 30 bilayer sample was prepared identically as previously described for the 5 bilayer samples. From cross sectional SEM imaging, this sample had a total thickness of 31.08 \pm 1.59 μ m (Figure 6B), resulting in a total thickness 5.0 x greater than that of the 5 bilayer sample (6.17 \pm 0.52 μ m), which was slightly smaller than expected

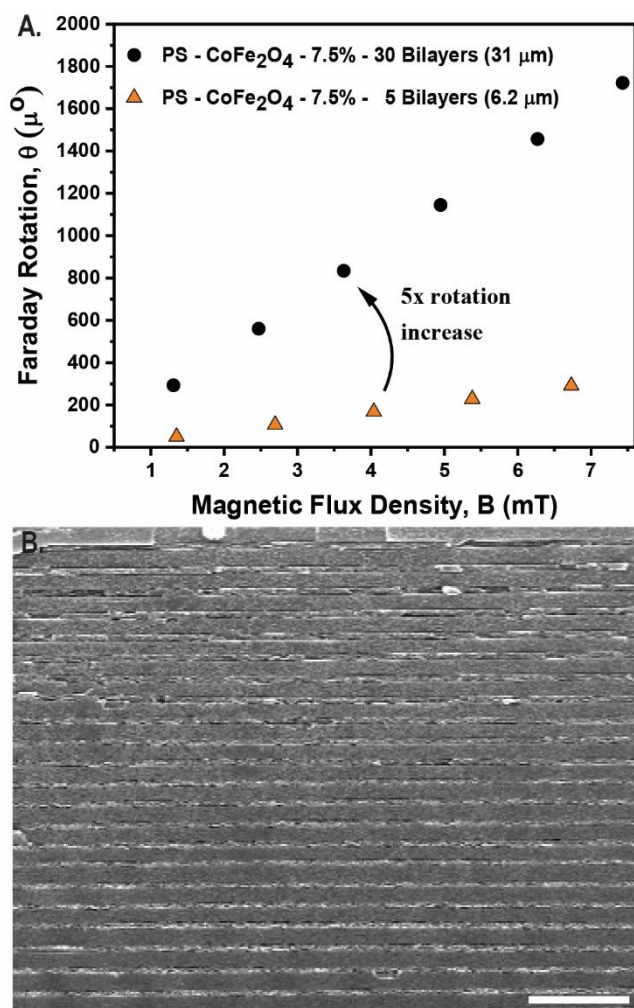


Figure 6. Demonstration of distributed Bragg-reflector architecture for increased total rotation. (A) Measurement of total Faraday rotation as a function of magnetic flux density in the 0–8 mT range for PS-CoFe₂O₄-7.5 wt% samples prepared with 5 bilayers (orange triangles) and 30 bilayers (black circles). (B) Cross sectional SEM of portion of 30-bilayer stack. Scale bar is 5 microns.

considering 6x the number of spin coating steps were employed in the preparation of this higher pathlength device. We attribute this difference in thickness to the natural curvature of the spin-coated film as a substantially thick (60 total layer) system is approached. Remarkably, the 30 bilayer sample showed a total rotation of 1722 μdeg at 740 mT, which is five-fold greater than that observed for the 5 bilayer sample. To our knowledge, this is the first example of a predictable and linear increase in rotation through a multi-layered film approach with a MO active polymer-nanoparticle composite.

4. Conclusion

In conclusion, we have demonstrated a new approach for the fabrication of processible MO active polymer-nanoparticle composites that enables predictable and tunable Verdet constants ($\sim 4.0 \times 10^3$ to 2.1×10^4 $^\circ/\text{Tm}$ at 1310 nm) that are up to ten-fold greater than commercial inorganic garnet rotators

through simple tuning of nanoparticle loading and composite thickness. By exchanging native oleic acid surface ligands for polymer compatible PS-COOH ligands, enhanced dispersion of primary NPs in a polystyrene matrix was observed up to 15.0 wt% NP loading, enabling simple preparation of polymer-nanoparticle films of tunable composition. Employing a distributed Bragg reflector inspired device architecture, reasonably thick samples could be prepared (~ 5 –6 μm), allowing sensitive measurement of Faraday rotation at weak fields (1–7 mT). We have observed an increase in Verdet constant with particle loading, with future work directed towards optimization of interparticle spacing to further elucidate particle-particle effects in tuning and enhancing composite Faraday rotation. Furthermore, a proportional increase in total rotation as a function of device thickness upon extending this work to thicker (~ 30 micron) systems was also shown, paving the way for scalable device fabrication with improved sensitivity. This seminal demonstration highlights the advantages of using polymer-nanoparticle composites as Faraday rotators in the NIR, and opens new possibilities for the fabrication of “plastic garnets” as low cost alternatives to commercial crystalline garnet materials for Faraday rotation.

Conflicts of interest

There are no conflicts to declare.

Acknowledgements

We gratefully acknowledge the Defense Advanced Research Projects Agency Microsystems Technology Office (DARPA MTO D16PC00192; DARPA MTO D17PC00302), the State of Arizona’s Technology and Research Initiative Fund (TRIF) and CIAN NSF ERC #EEC-082072 for financial support of this work, and N.G.P. acknowledges partial support from the European Union’s Horizon 2020 research and innovation programme under the Marie Skłodowska-Curie grant agreement No. 798409-HMST-PC.

Notes and references

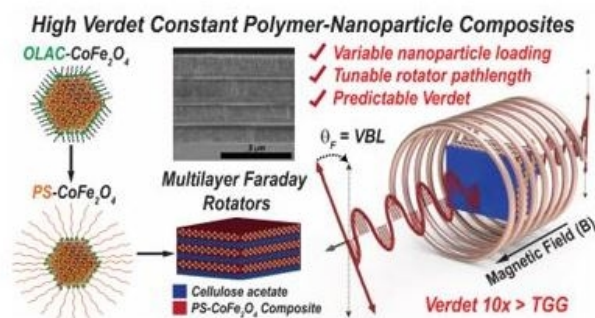
1. R. Bahuguna, M. Mina, J.-W. Tioh and R. J. Weber, *IEEE Transactions on Magnetics*, 2006, **42**, 3099–3101.
2. P. Zu, C. C. Chan, G. W. Koh, W. S. Lew, Y. Jin, H. F. Liew, W. C. Wong and X. Dong, *Sensors and Actuators B-Chemical*, 2014, **191**, 19–23.
3. M. Zayat, F. del Monte, M. P. Morales, G. Rosa, H. Guerrero, C. J. Serna and D. Levy, *Adv. Mater.*, 2003, **15**, 1809–1812.
4. S. Taccola, F. Greco, A. Zucca, C. Innocenti, C. d. J. Fernandez, G. Campo, C. Sangregorio, B. Mazzolai and V. Mattoli, *Acs Applied Materials & Interfaces*, 2013, **5**, 6324–6332.
5. R. M. Silva, H. Martins, I. Nascimento, J. M. Baptista, A. L. Ribeiro, J. L. Santos, P. Jorge and O. Frazao, *Applied Sciences-Basel*, 2012, **2**, 602–628.

6. J. Manuel Caicedo, O. Pascu, M. Lopez-Garcia, V. Canalejas, A. Blanco, C. Lopez, J. Fontcuberta, A. Roig and G. Herranz, *ACS Nano*, 2011, **5**, 2957-2963.
7. M. A. Schmidt, L. Wondraczek, H. W. Lee, N. Granzow, N. Da and P. S. J. Russell, *Adv. Mater.*, 2011, **23**, 2681-2688.
8. J. C. Suits, *IEEE Transactions on Magnetics*, 1972, **MAG8**, 95-8.
9. L. D. Barron, *Molecular Light Scattering and Optical Activity*, 2nd ed., Cambridge University Press, 2004.
10. A. K. Z. a. V. A. Kotov, *Studies in Condensed Matter Physics. Modern Magneto-optics and Magneto-optical Materials*, CRC Press, 1997.
11. R. V. Mikhaylovskiy, E. Hendry and V. V. Kruglyak, *Physical Review B*, 2012, **86**.
12. H. Majeed, A. Shaheen and M. S. Anwar, *Opt. Express*, 2013, **21**, 25148-25158.
13. D. E. Lacklison, G. B. Scott, H. I. Ralph and J. L. Page, *IEEE Transactions on Magnetics*, 1973, **MAG9**, 457-460.
14. B. Amirsolaimani, P. Gangopadhyay, A. P. Persoons, S. A. Showghi, L. J. LaComb, R. A. Norwood and N. Peyghambarian, *Opt. Lett.*, 2018, **43**, 4615-4618.
15. P. Gangopadhyay, R. Voorakaranam, A. Lopez-Santiago, S. Foerier, J. Thomas, R. A. Norwood, A. Persoons and N. Peyghambarian, *Journal of Physical Chemistry C*, 2008, **112**, 8032-8037.
16. V. Doormann, J. P. Krumme and H. Lenz, *J. Appl. Phys.*, 1990, **68**, 3544-3553.
17. P. Wang, I. Jeon, Z. Lin, M. D. Peeks, S. Savagatrup, S. E. Kooi, T. Van Voorhis and T. M. Swager, *J. Am. Chem. Soc.*, 2018, **140**, 6501-6508.
18. C.-K. Lim, M. J. Cho, A. Singh, Q. Li, W. J. Kim, H. S. Jee, K. L. Fillman, S. H. Carpenter, M. L. Neidig, A. Baev, M. T. Swihart and P. N. Prasad, *Nano Lett.*, 2016, **16**, 5451-5455.
19. A. Lopez-Santiago, H. R. Grant, P. Gangopadhyay, R. Voorakaranam, R. A. Norwood and N. Peyghambarian, *Optical Materials Express*, 2012, **2**, 978-986.
20. A. Lopez-Santiago, P. Gangopadhyay, J. Thomas, R. A. Norwood, A. Persoons and N. Peyghambarian, *Appl. Phys. Lett.*, 2009, **95**.
21. A. Miles, Y. Gai, P. Gangopadhyay, X. Wang, R. A. Norwood and J. J. Watkins, *Optical Materials Express*, 2017, **7**, 2126-2140.
22. V. Demir, P. Gangopadhyay, R. A. Norwood and N. Peyghambarian, *Faraday rotation of cobalt ferrite nanoparticle polymer composite films at cryogenic temperatures*, 2014.
23. H. C. Y. Yu, M. A. van Eijkelenborg, S. G. Leon-Saval, A. Argyros and G. W. Barton, *Appl. Opt.*, 2008, **47**, 6497-6501.
24. E. M. Moreno, M. Zayat, M. P. Morales, C. J. Serna, A. Roig and D. Levy, *Langmuir*, 2002, **18**, 4972-4978.
25. Z. H. Zhou, J. M. Xue, H. S. O. Chan and J. Wang, *J. Appl. Phys.*, 2001, **90**, 4169-4174.
26. H. Cui, M. Wang, W. Ren, Y. Liu and Y. Zhao, *J. Sol-Gel Sci. Technol.*, 2013, **66**, 512-517.
27. R. Garcia, M. Ramirez-del-Solar, J. M. Gonzalez-Leal, E. Blanco and M. Dominguez, *Mater. Chem. Phys.*, 2015, **154**, 1-9.
28. A. Lopez-Santiago, P. Gangopadhyay, J. Thomas, R. A. Norwood and N. Peyghambarian, San Jose, California, 2009.
29. R. B. Grubbs, *Polymer Reviews*, 2007, **47**, 197-215.
30. R. B. Grubbs, *J. Polym. Sci. Pol. Chem.*, 2005, **43**, 4323-4336.
31. L. A. Míinea, L. B. Sessions, K. D. Ericson, D. S. Glueck and R. B. Grubbs, *Macromolecules*, 2004, **37**, 8967-8972.
32. Q. Dai, D. Berman, K. Virwani, J. Frommer, P.-O. Jubert, M. Lam, T. Topuria, W. Imaino and A. Nelson, *Nano Lett.*, 2010, **10**, 3216-3221.
33. Q. Dai and A. Nelson, *Chem. Soc. Rev.*, 2010, **39**, 4057-4066.
34. R. Hong, N. O. Fischer, T. Emrick and V. M. Rotello, *Chem. Mater.*, 2005, **17**, 4617-4621.
35. B. D. Korth, P. Keng, I. Shim, S. E. Bowles, C. Tang, T. Kowalewski, K. W. Nebesny and J. Pyun, *J. Am. Chem. Soc.*, 2006, **128**, 6562-6563.
36. K. Pei Yuin, S. Inbo, B. D. Korth, J. F. Douglas and J. Pyun, *ACS Nano*, 2007, **1**, 279-292.
37. M. M. Bull, W. J. Chung, S. R. Anderson, S. J. Kim, I. B. Shim, H. J. Paik and J. Pyun, *J. Mater. Chem.*, 2010, **20**, 6023-6025.
38. B. D. Korth, P. Y. Keng, I. Shim, C. Tang, T. Kowalewski and J. Pyun, in *Nanoparticles: Synthesis, Stabilization, Passivation, and Functionalization*, American Chemical Society, 2008, vol. 996, ch. 20, pp. 272-285.
39. P. Wang, S. B. Lin, Z. Lin, M. D. Peeks, T. Van Voorhis and T. M. Swager, *J. Am. Chem. Soc.*, 2018, **140**, 10881-10889.
40. P. Gangopadhyay, G. Koeckelberghs and A. Persoons, *Chem. Mater.*, 2011, **23**, 516.
41. P. Gangopadhyay, R. Voorakaranam, A. Lopez-Santiago, S. Foerier, J. Thomas, R. A. Norwood, A. Persoons and N. Peyghambarian, *The Journal of Physical Chemistry C*, 2008, **112**, 8032-8037.
42. P. Gangopadhyay, S. Foerier, G. Koeckelberghs, M. Vangheluwe, A. Persoons and T. Verbiest, *Proc. SPIE*, 2006, 63310Z.
43. L. T. Lu, N. T. Dung, L. D. Tung, C. T. Thanh, O. K. Quy, N. V. Chuc, S. Maenosono and N. T. K. Thanh, *Nanoscale*, 2015, **7**, 19596-19610.
44. A. López-Ortega, E. Lottini, C. d. J. Fernández and C. Sangregorio, *Chem. Mater.*, 2015, **27**, 4048-4056.
45. B. Y. Kim, I.-B. Shim, Z. O. Araci, S. S. Saavedra, O. L. A. Monti, N. R. Armstrong, R. Sahoo, D. N. Srivastava and J. Pyun, *J. Am. Chem. Soc.*, 2010, **132**, 3234-3235.
46. B. Y. Kim, I.-B. Shim, O. L. A. Monti and J. Pyun, *Chem. Commun.*, 2011, **47**, 890-892.
47. X. Wang, R. D. Tilley and J. J. Watkins, *Langmuir*, 2014, **30**, 1514-1521.
48. O. Louant, V. Liégeois, T. Verbiest, A. Persoons and B. Champagne, *The Journal of Physical Chemistry C*, 2017, **121**, 15348-15352.
49. T. S. Kleine, L. Ruiz Diaz, K. M. Konopka, L. E. Anderson, N. G. Pavlopolous, N. P. Lyons, E. Tae Kim, Y. Kim, R. S. Glass, K. Char, R. A. Norwood and J. Pyun, *One Dimensional Photonic Crystals Using Ultrahigh Refractive Index Chalcogenide Hybrid Inorganic/Organic Polymers*, 2018.
50. S. Gazzo, G. Manfredi, R. Pötzsch, Q. Wei, M. Alloisio, B. Voit and D. Comoretto, *J. Polym. Sci., Part B: Polym. Phys.*, 2016, **54**, 73-80.
51. P. Tao, Y. Li, A. Rungta, A. Viswanath, J. Gao, B. C. Benicewicz, R. W. Siegel and L. S. Schadler, *J. Mater. Chem.*, 2011, **21**, 18623-18629.
52. D. A. Smith, Y. A. Barnakov, B. L. Scott, S. A. White and K. L. Stokes, *J. Appl. Phys.*, 2005, **97**, 10M504.

Polymer and Magnetic Nanoparticle Composites with Tunable Magneto-Optical Activity: Role of Nanoparticle Dispersion for High Verdet Constant Materials

Pavlopoulos, N. G.^{a,b}; Kang, K. S.^a; Holmen, L.N.^a; Lyons, N.P.^c; Akhondi, F.^c; Carothers, K.J.^a; Jenkins, S.L.^c; Lee, T.^a; Kochenderfer, T.M.^a; Phan, A.^a; Phan, D.^d; Mackay, M.E.^d; Shim, I.^e; Char, K.^e; Peyghambarian, N.^c; LaComb L.^c; Norwood, R.A.^c; Pyun, J.^a

The critical role of nanoparticle dispersion on composite Faraday rotator activity was studied, revealing new routes for fabricating “*plastic garnets*” as low cost alternatives to existing inorganic materials for optical isolation and magnetic sensing



169x111mm (96 x 96 DPI)